

Article

An Anchoring Groove Technique to Enhance the Bond Behavior between Heat-Damaged Concrete and CFRP Composites

Rajai Al-Rousan *  and Mohammad AL-Tahat

Department of Civil Engineering, Jordan University of Science and Technology, Irbid 22110, Jordan; mftahat16@eng.just.edu.jo

* Correspondence: rzalrousan@just.edu.jo; Tel.: +962-799887574

Received: 18 November 2020; Accepted: 30 November 2020; Published: 7 December 2020



Abstract: This experimental study was conducted to evaluate the effectiveness of using carbon fiber-reinforced polymer (CFRP) composites with special anchoring grooves, specifically in terms of the ability of the concrete–CFRP bond to withstand elevated temperatures. The obtained findings of this experiment clearly highlighted the effectiveness of the direction of the anchoring grooves on the behavior of the concrete–CFRP bonding area. The results also showed that high temperatures lessen the bond’s strength and the ultimate slippage. On the other hand, this study showed that increasing the length of the CFRP sheet resulted in enhancement of the bond’s strength and slippage. When exposed to temperatures above 500 °C, the structures’ residual splitting and compression strength decreased significantly, resulting in the bond’s strength reducing to 67% and the slippage to 19%, with respect to the control samples. In the non-grooved and vertically grooved beams, the CFRP–concrete bond showed a skin-peeling type of failure. It appeared, also, that the temperature and the number of anchored grooves significantly affected the bonding area of the surface; as the surface was exposed to failure in adhesion, more concrete remained attached to the CFRP composite, signifying a stronger attachment.

Keywords: bond-slip behavior; anchoring groove; elevated temperature

1. Introduction

Concrete has been the most extensively used material for structures for decades. Nevertheless, concrete is classified as a brittle material, with a low strain limit and tensile strength capacity. There have been ongoing efforts to overcome these deficiencies using several strategies. The utilization of fibers in structural concrete elements began in the 1970s because of their ability to improve the mechanical properties of concrete. Broad examinations have now been completed on the utilization of various types of fibers for enhancing the concrete mechanical properties of structures. Nowadays, carbon fiber-reinforced polymer materials (CFRPs) are considered the main strengthening and rehabilitation composite materials of shear or in flexure-deficient reinforced concrete structures [1–5]. The quality of the reinforcement by CFRPs is mainly governed by the behavior of the CFRP–concrete bond. When this bond is not strong enough, de-bonding occurs, which is a disadvantageous brittle failure [6]. Research has been conducted to study the behavior of the CFRP–concrete bond-slip and its mode of failure at the adhered elements. These studies have focused on the concrete tensile and compressive strengths [7,8], the dimensions of the CFRP composites [9,10], hole configurations [11], preparation and roughness of the concrete bonded surface [12], and the CFRP composite anchorage system [13]. De-bonding failure appears in many forms. The separation of the concrete cover and intermediate induced cracks are examples of the most frequently occurring de-bonding failures due to excessive external loads [6,7].

To resolve the issue of de-bonding failure, the majority of design codes [14,15] require setting the strain of FRP laminates within strict limits, which consequently minimizes the use of the laminates' tensile capacity.

In certain cases, techniques of surface preparation (or treatment) have been advised by the American Concrete Institute (ACI) [16] and the International Concrete Repair Institute [17] to be used to enhance the quality of the FRP–concrete bonding area to avoid de-bonding. Among these techniques is the method of blasting by abrasives and water, which enhances the concrete's superficial roughness through the removal of the mortar's upper layer. This method was used in research conducted by De Lorenzis and Nanni [18]. They found that the strength of the FRP–concrete increased considerably when the bonding area was prepared (or roughened) using a water jet and sandblasting and then adding notches to the concrete surface. In addition, the mode of failure became rupture instead of de-bonding. Toutanji and Ortiz [19] realized that the water jetting method was more effective than sandblasting in strengthening the bonding area by improving the surface roughness of the concrete. In addition, Chajes et al. [20] concluded that utilizing mechanical abrading to roughen the concrete surface resulted in an enhancement of 10%, according to the former team, in the ultimate load; the second team found that structural durability was increased too. Biscaia and Silva [21] used the single sheet test to investigate the effect of sandblasting on the ultimate load of strengthened-by-FRP structures. The test results showed that the ultimate level of load was lessened when the sandblasting was deeper and increased when light sandblasting was used. Iovinella et al. [22] studied the effectiveness of bush-hammering and sandblasting on the concrete–FRP bond. They found that this method improved the strength of the bond by 30–50%.

The quality of prepared concrete surfaces has been of great concern to all practitioners of conventional methods of surface treatment. This is because it is impossible to construct sample elements of the same roughness, because of the lack of experienced workers able to perform surface treatments. Poorly prepared concrete surfaces result in weak bonding [23], even if workers abide by the method and the strict specifications set by the International Concrete Repair Institute [17] regarding the roughness of the concrete surface. Therefore, roughness quality remains an issue due to the absence of reliable codes and measurements for surface roughness.

Therefore, a modern surface treatment method has been introduced to replace the conventional methods, involving externally bonded reinforcement on grooves [24,25], known as the grooving method [26,27]. The use of grooves on the flexural loading zone, transversally directed grooves, and the parameters of the grooves have been studied recently. The mechanism of the interlocking effect of transverse grooving was first proposed by Jiang et al. [28] and further studied by Chen et al. [29]. The grooving system is based on drilling grooves in the concrete transversely, longitudinally, or diagonally. Next, the grooves are filled with an adhesive material (epoxy). Finally, the FRP material is mounted and adhered onto the grooves. According to Mostofinejad and Mahmoudabadi [30], upon applying four-point bending loads on reinforced concrete (RC) beams reinforced by externally bonded FRP laminates, the grooving method succeeded in enhancing the ultimate load and prevented de-bonding failure. An experimental study was undertaken by Hosseini and Mostofinejad [30,31], wherein they applied the single shear test to grooved samples. They found that enlarging the longitudinal grooves' width resulted in enhancement of the bond stiffness, while the in-between slip was minimized such that there was no noticeable change upon raising the grooves' depth. The grooving method ensures good-quality bonding, resolves the de-bonding failure problem, and enhances the ultimate load by 10 to 15% [24]. The grooving quality depends mainly on the grooves' length, width, and clearance.

However, the lack of literature about the grooving system remains an obstacle that hinders the use of the method. There is a lack of information about the behavior of the FRP–concrete bond when impacted by grooves on the flexural loading zone, transversally directed grooves, and the parameters of the grooves (namely the length, width, and clearance). Therefore, more experimental studies are needed to better understand the grooving method. According to Mostofinejad and Mahmoudabadi [26],

the grooving method enhances the FRP–concrete bonding area, enhancing the ultimate load. Deep sand blasting, as observed by Biscaia and Silva [32], reduced the ultimate load due to the emergence of weak spots on the surface of the concrete. In addition, the majority of the current methods of bonding in RC structures strengthened with externally bonded FRP materials have omitted the role of grooves in enhancing the ultimate load [33–36]. Therefore, there is a need to develop a design method to anticipate the ultimate load when using transversal grooves.

Concrete collapses when exposed to temperatures exceeding 500 °C. This is due to the variation in the concrete components' inhomogeneous volume, decomposition of cement hydration products, and the creation of vapor pressure beyond a temperature of 550 °C [37]. A number of researchers have stated that heat-damaged concrete elements suffer a drastic decrease in their elasticity modulus and their strength, in addition to a detachment of the bond with the embedded reinforcing steel [38,39]. Additionally, the concrete spalls, cracks, and skin-alters when exposed to temperatures exceeding 400 °C [37]. In order to restore the strength capacity of heat-damaged elements, particularly flexural ones, reliable reinforcing composite materials need to be utilized, such as CFRP laminates.

Therefore, thorough studies are needed to quantify and investigate the impact of excessive heat on the bonds, the geometric parameters of the CFRP composites, and the concrete's type and strength. This could help practitioners to specify an adequate area of CFRP–concrete bonding needed to avoid or delay bond failure in the case of fire attacks. A well-designed CFRP–concrete bond plays a role in restoring the load capacity of the damaged elements by transferring the developed stresses from the concrete to the CFRP materials. The efficiency of this load-restoring process relies mainly on the strength of the CFRP–concrete bond, adding to the mechanical and geometric characteristics of the material used in the repair and the quality of the epoxy. A number of researchers have found that, before repairing or strengthening a concrete element with CFRP laminates, it is of the utmost importance to perform a concrete surface preparation process to attain the best results.

This work is intended to investigate the effectiveness of drilled grooves in a concrete surface on the length and the width of the CFRP reinforcement sheets, aiming to address the shortage of available studies in this field. This work aimed to investigate the impact of groove direction on the behavior of the concrete–FRP bond. The bond's behavior was examined when exposed to high temperatures, a change in the groove direction, and a change in the length of the bond. Next, the specimens were tested using the pull-off method. After this, the last step was to utilize a universal testing machine in which a special flexure was fixed to graphically plot the relationship between the bond's stresses and strains.

2. Description of the Experimental Program

2.1. Test Specimens

Seventy-two (two from each type with a percentage error of less than 5% for both ultimate bond force and corresponding slippage) concrete prisms, with dimensions of 150 × 150 × 200 mm, were casted. The sample was divided into three groups. Each group was designated by characters (letters and numbers) that represented the temperature (T) (23, 250, 500, or 750 °C); the direction of the grooves (D) (0: None, V: Vertical, or H: Horizontal); the length of the bonded CFRP sheet (L_f) (65, 90, or 115 mm); and the CFRP sheet's width of bonding (b_f) of 90 mm; as illustrated in Figure 1 and stated in Table 1.

2.2. The Properties of the Materials

The concrete mixture utilized to cast the prism specimens was in compliance with the ACI mix design code [40]. The mix contained ordinary cement (Portland, Type I), fresh water (tap water), and squashed coarse and fine aggregates, so as to attain a 28-day compressive strength of 50 MPa and a tensile strength of 4.31 MPa, in addition to an 80 mm slump (Table 2). To prepare the specimens, both the CFRP sheets (SikaWrap® -300 C, Sika Group, Baar, Switzerland) and the adhesive epoxy of

(Sikadur[®]-330, Sika Group, Baar, Switzerland), with a glass transition temperature of 58 °C, were used. Table 3 shows the manufacturer’s specifications of both the CFRP composite sheets and the adhesive material (epoxy).

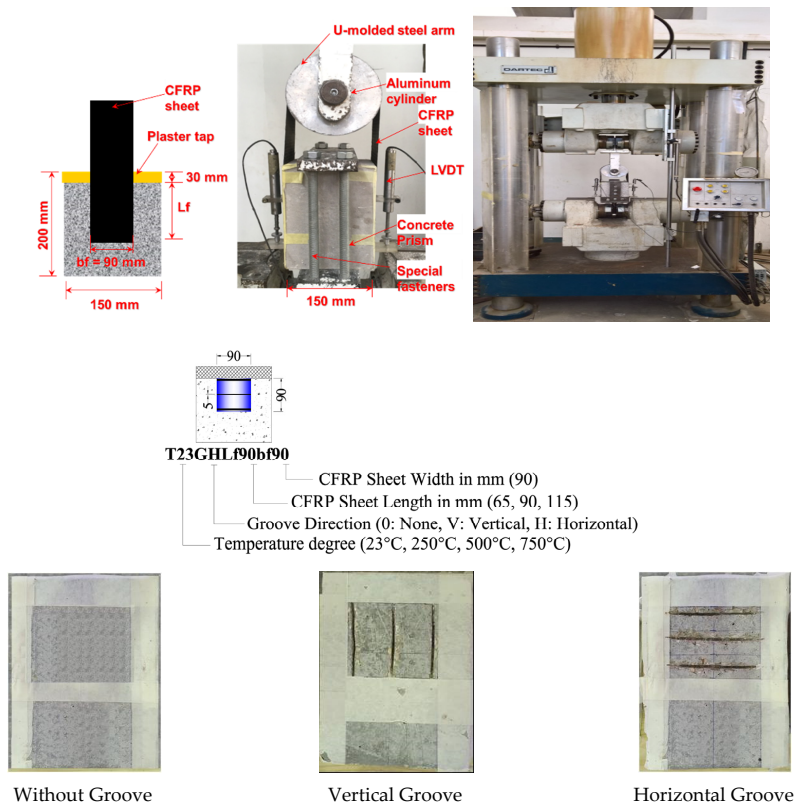


Figure 1. Specimen layout and test setup.

2.3. Heat Treatment Method

The samples were heat-treated for 120 min at temperatures ranging from 250 to 750 °C in a special furnace. Then, they were left in the furnace to cool down. The furnace used in this work was an electric type, with electronic control of the temperature possible up to 1200 °C. The time of exposure is shown in Figure 2.

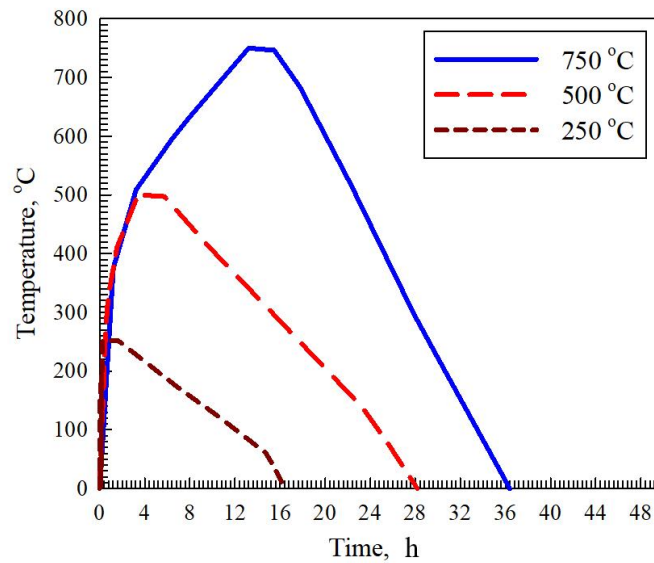


Figure 2. The time-temperature schedule.

Table 1. Specimen designation and results.

Designation	T, °C	Groove Direction	Lf, mm	Load, kN	Slippage, mm	Stiffness, kN/mm	Toughness, kN/mm	
T23GNLf65bf90	23	None	9.0	9.0	0.171	213	1.38	
T23GNLf90bf90			10.6	10.6	0.201	267	1.97	
T23GNLf115bf90			12.5	12.5	0.238	326	2.78	
T23GVLf65bf90		Vertical	Vertical	11.4	11.4	0.233	263	2.38
T23GVLf90bf90				13.4	13.4	0.274	328	3.37
T23GVLf115bf90				15.7	15.7	0.321	404	4.71
T23GHLf65bf90			Horizontal	21.4	21.4	0.405	284	7.78
T23GHLf90bf90				24.9	24.9	0.470	356	10.77
T23GHLf115bf90				29.1	29.1	0.546	441	14.86
T250GNLf65bf90	250	None	7.9	7.9	0.169	188	1.19	
T250GNLf90bf90			9.3	9.3	0.198	235	1.69	
T250GNLf115bf90			10.9	10.9	0.235	288	2.39	
T250GVLf65bf90		Vertical	Vertical	9.9	9.9	0.205	260	1.83
T250GVLf90bf90				11.7	11.7	0.242	324	2.59
T250GVLf115bf90				13.7	13.7	0.283	399	3.63
T250GHLf65bf90			Horizontal	18.6	18.6	0.357	280	5.98
T250GHLf90bf90				21.7	21.7	0.415	351	8.28
T250GHLf115bf90				25.4	25.4	0.482	435	11.43
T500GNLf65bf90	500	None	5.2	5.2	0.151	147	0.70	
T500GNLf90bf90			6.1	6.1	0.178	184	0.99	
T500GNLf115bf90			7.2	7.2	0.210	225	1.40	
T500GVLf65bf90		Vertical	Vertical	6.5	6.5	0.166	211	0.97
T500GVLf90bf90				7.7	7.7	0.195	264	1.37
T500GVLf115bf90				9.0	9.0	0.229	325	1.92
T500GHLf65bf90			Horizontal	12.3	12.3	0.262	251	2.88
T500GHLf90bf90				14.3	14.3	0.305	314	3.99
T500GHLf115bf90				16.7	16.7	0.354	389	5.51
T750GNLf65bf90	750	None	2.9	2.9	0.139	113	0.37	
T750GNLf90bf90			3.5	3.5	0.164	142	0.52	
T750GNLf115bf90			4.1	4.1	0.193	174	0.73	
T750GVLf65bf90		Vertical	Vertical	3.7	3.7	0.144	138	0.48
T750GVLf90bf90				4.4	4.4	0.169	172	0.68
T750GVLf115bf90				5.1	5.1	0.199	212	0.95
T750GHLf65bf90			Horizontal	7.0	7.0	0.162	231	1.01
T750GHLf90bf90				8.1	8.1	0.188	290	1.40
T750GHLf115bf90				9.5	9.5	0.218	359	1.93

Two specimens were casted for each tested parameter; T: temperature; GN: without groove; GV: vertical groove; GH: horizontal groove; Lf: carbon fiber-reinforced polymer (CFRP) bonded length; bf: CFRP bonded width.

Table 2. Mixture proportions of the concrete.

Material	Mixture (50 MPa)
Cement	422 kg/m ³
Coarse Aggregate	706 kg/m ³
Fine Aggregate	621 kg/m ³
Water	147.6 kg/m ³
Superplasticizer	As required

2.4. Preparation of Specimens

Based on the study parameters (Figure 1 and Table 1), the specimens were split into groups. The concrete blocks had been casted for 24 h before they were de-molded and cured in a tank of lime-saturated water for 28 days [40]. Next, grooves (10 mm deep, 90 mm long) were drilled into the blocks, with a distance between the grooves of 40 mm, center to center [41]. After drilling, the concrete surface preparation, to achieve good-quality adhesion, was carried out by cleaning the grooves using a vacuum cleaner and a volatile liquid, to minimize the moisture content on the concrete surface. Some

of the grooves were vertical, while others were horizontal. On every block surface, the bonding surface, where the CFRP sheets were to be attached, was marked (Figure 3), and the sheets were cut to the desired dimensions. Next, the preparation process of the epoxy was carried out by using an electric mixer to mix the epoxy's part A and part B in two parts, at a ratio of 4:1, slowly for four minutes, followed by fast mixing for one minute, to attain a uniformly mixed paste. Then, the prepared paste was spread on each sample's marked areas (Figure 3). To prevent the concentration of stresses, an area was left without bonding 30 mm away from the top edge. Later, all of the study samples were left at ambient temperature for a week prior to experimentation (Figure 3).

Table 3. Physical and mechanical properties of the Sika CFRP sheet and Sika epoxy.

Sika CFRP Sheet	Fabric Thickness	0.167 mm (based on fiber content)
	Fiber Density	1.82 g/cm ³
	Tensile Modulus	230,000 N/mm ²
	Tensile Strength	4000 N/mm ²
	Break Elongation	1.7%
Sika Epoxy	Tensile Strength	30 N/mm ² (7 days at +23 °C)
	E-Modulus	Flexural: 3800 N/mm ² (7 days at +23 °C) Tensile: 4500 N/mm ² (7 days at +23 °C)
	Break Elongation	0.9% (7 days at +23 °C)

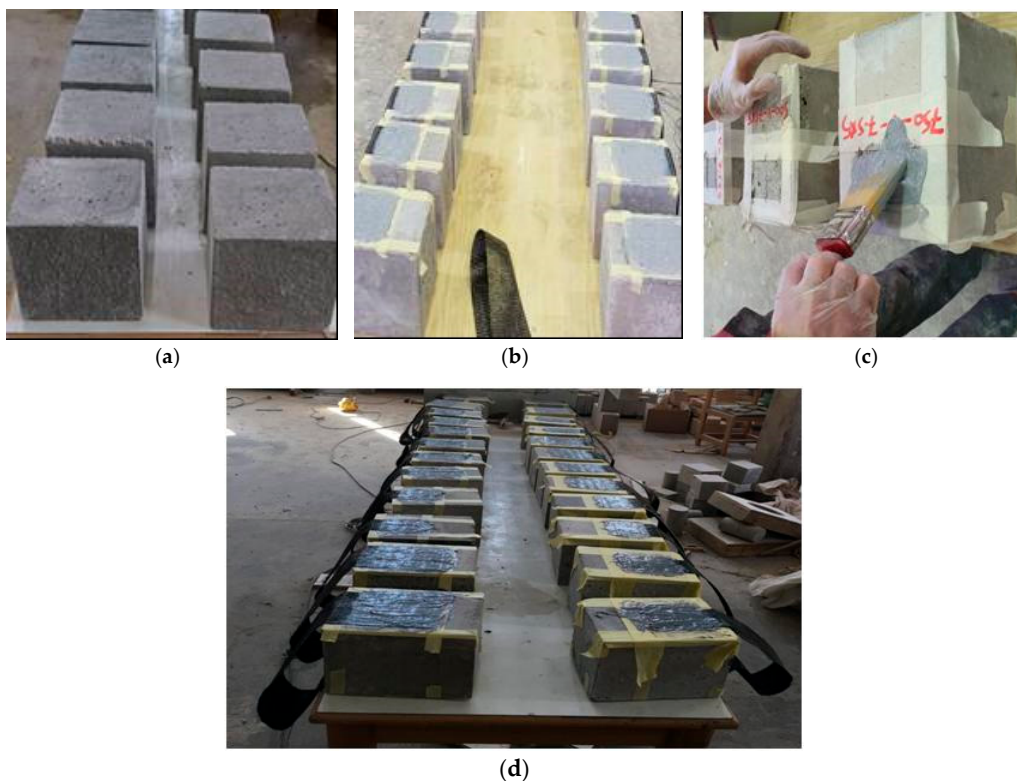


Figure 3. Bonding of the CFRP sheets (a) without surface preparation; (b) smooth surface preparation; (c) preparation of grooves; (d) specimens with different CFRP composite sheet lengths and widths.

2.5. Test Procedure

As in previous studies, the blocks were subjected to double shear tests [8–10,12], utilizing a universal testing machine, with a hydraulic jack attached to a stiff steel frame system, as illustrated in Figure 1. The blocks were supported on one side, while the other side was loaded by vertical force, thus applying shear force on the bond interface. To determine the compressive strength of each batch, six 100 × 200 mm concrete cylinders were prepared according to ASTM C39 [40]. In order to level their surfaces, the cylinders were wrapped with sulfur before they were subjected to the testing

procedures. The testing machine was set to generate the tensile force (Figure 1) using a U-shaped arm of steel, mounted on a cylinder of aluminum. The cylinder was gradually pulled until the CFRP sheets de-bonded. Two linear variable differential transformers (LVDT) were installed on the CFRP sheets to monitor their slippage (relative displacement) from concrete. It is worth mentioning that the LVDT instruments were attached to the sheets by two connected glass plates; one was pasted to the concrete and the other to the measuring instruments.

3. Results and Discussion

3.1. Effect of Elevated Temperatures on Strength Residuals

The impact of elevated temperatures on the casted specimens is shown in Figure 4, which depicts the residuals for splitting and compressive strength versus applied temperature. The response showed a similar trend, characterized by a minor decrease at a temperature of 250 °C and by a major decrease at higher temperatures. The clear consequence of high temperatures above 250 °C on both strengths was the decomposition of the cement when exposed to temperatures above 500 °C and/or the emergence of cracks due to heat. Map-shaped cracking emerged due to escalated heat and this increased with the increase in the temperature, whereas the surface showed no visual alteration. Referring to Figure 4, the residual strengths (compressive, splitting) decreased by 95% and 91% at 250 °C and by 44% and 27% at 750 °C.

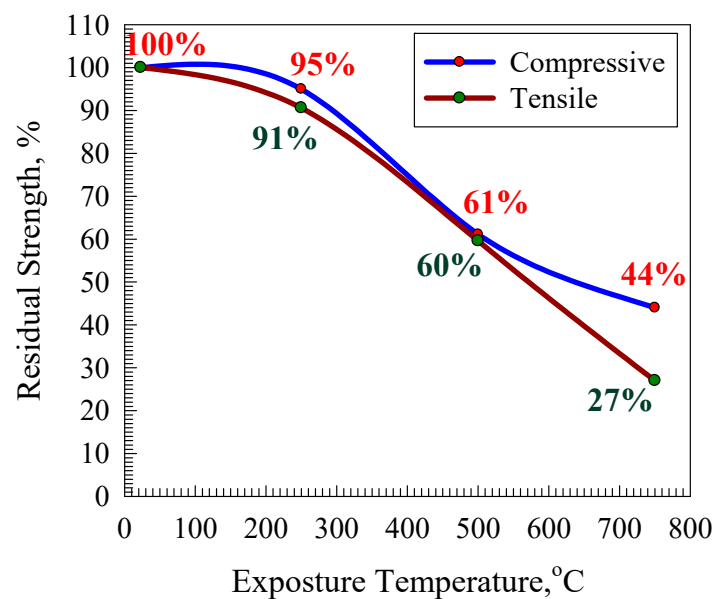


Figure 4. Residuals for compressive and splitting strengths.

3.2. Mode of Failure

The majority of the test specimens had either a de-bonding mode of failure at the concrete–CFRP interface of adhesion (failure mode I) or a peel-off mode of failure at the same area, where the concrete peeled off in different thicknesses, leaving behind varying amounts of concrete hooked to the sheets (failure mode II) (Figure 5a). While applying the loads, cracking with a popping sound was produced at the first instance of failure. When the applied load was further elevated, the cracks continued to emerge, with louder sounds. Some of these cracks began emerging at the edge of the CFRP sheet and stretched to the specimen's top surface, leading to peeling of the concrete at the end of loading. Later, the CFRP sheet de-bonded at the end furthest from the loading end. As a consequence, the CFRP sheet fully detached, leading to complete failure, as shown in Figure 5a. This failure was brittle and related to high energy release, which occasionally causes CFRP sheet longitudinal splitting. The duration of the de-bonding process was affected by the CFRP bonded length, surface preparation, drilling

diameter, and the temperature. With reference to Figure 5a, it can be seen that the mode of failure was adhesive (failure mode I) in the non-grooved and vertically grooved specimens, at the CFRP–concrete interface. As for the horizontally grooved samples, failure mode II took place, as the concrete peeled off at a thickness similar to the concrete layer. Post the peel-off failure, varying amounts of the broken-off concrete remained on the CFRP sheet (Figure 5a).



Figure 5. Typical mode of failure. (a) Specimens with different drilling diameters; (b) specimens with different CFRP bonded lengths; (c) specimens with different temperature degrees.

Figure 5b depicts that the non-grooved samples' mode of failure mode was adhesive failure. Further, when the grooves increased, more concrete remained hanging onto the reinforcing sheet at the surface of the failed adhesion. This is a strong indication of the enhanced strength of the bonding. It is worth noting that the grooved specimens' bond strength, at failure, was greatly enhanced with respect to the controls. In addition, the direction of grooves greatly affected the failure mode. All of the specimens, whether they had vertical, horizontal, or no grooves, encountered failure mode I with

an adhesion failure at the interface of the concrete–CFRP sheets; then, huge peeling-off occurred at the large un-bonded top portion of the concrete (Figure 5a).

The length of the bonded CFRP sheet directly affects the failure time (Figure 5b); an increase in the length of the bonded CFRP leads to an increase in the warning period prior to final bond failure. On the contrary, only a small period of pre-failure warning was provided when using CFRP bonded with the shortest length. Post the occurrence of failure, the bonding area retained its roughness, while the remaining bonded area was free of adhesives. Finally, the thickness of the concrete interface peel-off was enhanced as the temperature increased, as illustrated in Figure 5c.

3.3. Bond Force–Slippage Responses

Figure 6 illustrates the responses that represent the relationship between the strength of the bond versus the behavior of the slip (the slippage and how it is impacted by the direction of grooving and the dimensions (the width and the length) of the bonded sheet of CFRP). The response was split into two sections: firstly, from the instant before loading (zero load) to the point of the CFRP sheet's de-bonding (stabilization of the behavior), in which a rapid increase in the load is met with a slight increase in slippage. It is worth mentioning that the response slope began to vary due to the nonlinear behavior of the CFRP–concrete interface region. Secondly, the response indicates a rapid increase in slippage where the load is nearly constant. This appears when the CFRP begins to de-bond from the concrete surface and is due to the lessening of the specimens' stiffness caused by the nonlinear behavior of the CFRP–concrete interface area, causing the CFRP sheets to endure the exerted load. Figure 6 indicates that the slope of both sections of the response increased considerably with the increase of the length of the CFRP sheet and groove direction. On the other hand, an increase in the temperature resulted in a significant slope decrease. In the first section and the ultimate slippage of the force–slippage response, the temperature strongly influenced the relationship of the force and the slippage, whereas the slope of the first stage increased more at low temperatures than at excessive temperatures. Further, the slope, in the second section of the response, stayed almost constant, as depicted in Figure 6.

At different temperatures, the curves showed similar behavior, depicted as a slight decrease in bond strength at a temperature of 250 °C, followed by a major reduction at higher temperatures. In addition, the slip—at failure—decreased at higher temperatures, because high temperatures cause the concrete to soften. The critical response of the bond at temperatures exceeding 500 °C is possibly due to a considerable reduction in strength. The improved adhering of the well-prepared epoxy to a well-treated concrete surface was probably the reason behind the enhancement in the bond strength, particularly in the pulled-off samples, at a temperature of 250 °C. It must be stated that the enhancement in the epoxy's adhering quality to a well-treated concrete constrained the reduction of the splitting and compressive strengths to below 9%. The reinforcing of the concrete structures by anchored grooves with long CFRP sheets improved the behavior of the bond force and the slippage post the initial de-bonding of the CFRP from the concrete surface.

3.4. Ultimate Bond Force and Slippage

The experimental results are shown in Table 1. The values of the tested specimens' ultimate bond force and corresponding slippage versus the configuration of the CFRP composites (Figure 7) were normalized with respect to an unheated (control), non-grooved specimen. Referring to Figure 7a, it appears that the bonded CFRP sheet's length increased by 38% (at 90 mm) and 77% (at 115 mm), while the ultimate bond force increased by 18% and 38%, respectively, with an increase rate of 1.52% for each 1 mm of CFRP bonded length. The average percentage of the improvement in the ultimate slippage was 20 and 39% for a CFRP sheet bonded length of 90 and 115 mm, respectively, as shown in Figure 7b. This percentage is 1.08 times better than the ultimate load percentage.

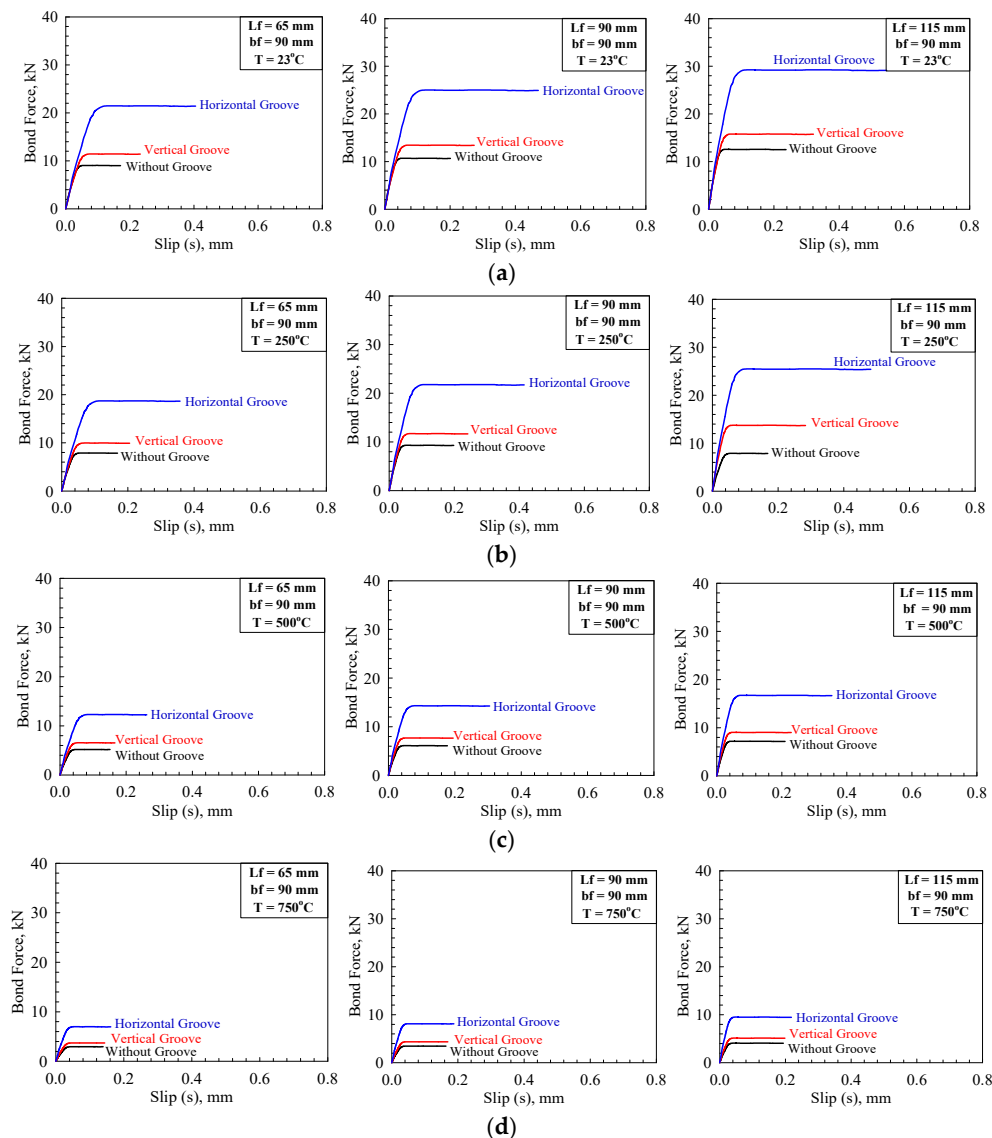


Figure 6. Typical bond-slip responses. (a) 23 °C; (b) 250 °C; (c) 500 °C; (d) 750 °C.

For the specimens with anchored grooves, both the ultimate bond force and corresponding slippage were normalized as per the control, non-grooved sample. Figure 7 presents the obtained results graphically. These indicate that the bond force and slippage were twice as affected by the anchored grooves system as by the length of the CFRP bonded sheet. Figure 7a indicates that the ultimate bond force was enhanced by around 63 and 26% for horizontally and vertically grooved specimens, respectively. The ultimate slippage was enhanced (Figure 7b) by 36 and 69% for vertical and horizontal grooves, respectively. These percentages are 1.15 times the ultimate bond force percentage. Thus, horizontally anchored CFRP beams showed a fantastic ductile failure mode and major enhancement in both the ultimate bond force and corresponding slippage.

Figure 7a clarifies the temperature's impact on the ultimate bond force and slippage, compared to specimens treated at room temperature (23 °C). Figure 7a indicates that the ultimate bond force reduced by 12, 42, and 63% for specimens treated at temperatures of 250, 500, and 750 °C, respectively, with an average reduction in the ultimate bond force of 0.082% for each 1 °C. As for the temperature's effect on slippage, the specimens' ultimate slippage (Figure 7b) was reduced by 1, 12, and 19% for specimens treated at temperatures of 250, 500, and 750 °C, respectively, with an average reduction in the ultimate slippage of 0.021% per 1 °C, where this percentage is 0.25 times the ultimate bond force percentage. The due-to-temperature degradation of the ultimate bond force and slippage shows that the bond

strength is governed by the mode of failure; however, high temperatures increase the slippage and the bond force to considerably higher concrete thicknesses. This increase in the concrete thickness could be due to the decrease in the aggregate's shear strength when exposed to extremely high temperatures. The variation in the ultimate slippage and bond force post being exposed to temperature degrees above 500 °C could be due to the enhancement in the bond between the concrete substrate and CFRP, as this bond was further roughened by heat-cracking and was combined with a higher reduction in the shear strength of the concrete. The decay in shear strength with increasing temperature caused full peeling-off in the unbonded top portion of the concrete, especially at temperatures of more than 500 °C.

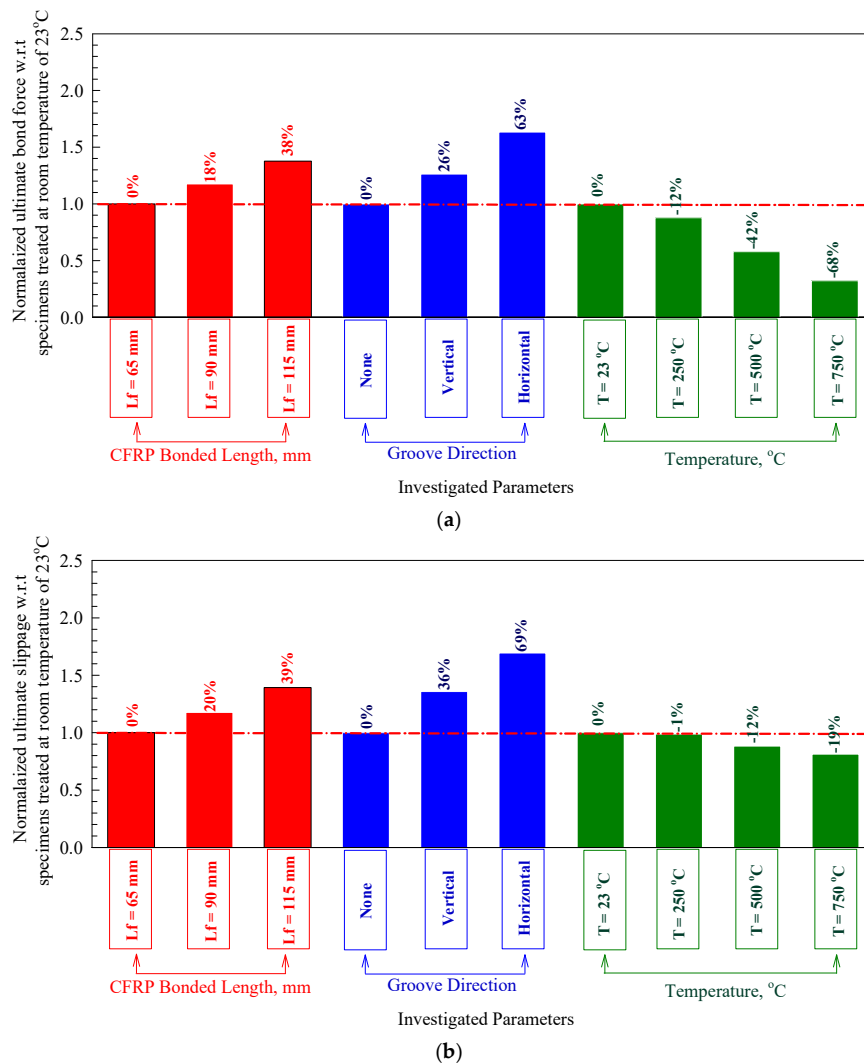


Figure 7. Normalized ultimate bond force and slippage. (a) Ultimate bond force; (b) ultimate slippage.

3.5. Stiffness

In the curve of the bond force vs. slippage, the slope of the first stage, the stage before the CFRP de-bonding, demonstrated elastic stiffness. For the purpose of comparison, each strengthened-by-CFRP test sample's stiffness was normalized according to the control non-grooved specimen, as depicted in Figure 8. Figure 8 shows that the increase in the length of the CFRP sheet was 38% (90 mm) and 77% (115 mm), enhancing the stiffness by 25 and 54%, respectively, with an enhancement rate of 1.08% per 1 mm of CFRP bonded length. Further, the average enhancement percentages in the stiffness of the grooved specimens were 23 and 27% for vertical and horizontal groove directions, respectively. Finally, the average percentages of reduction were 12, 31, and 47% for specimens treated at temperatures of 250, 500, and 750 °C, respectively, with an average reduction in ultimate bond force of 0.094% per 1 °C.

These findings highlight that utilizing the CFRP sheet technique and anchored horizontal grooves is very advantageous in restoring the specimen integrity to its original status before CFRP de-bonding and after reaching its ultimate bond force due to exposure to excessive heat.

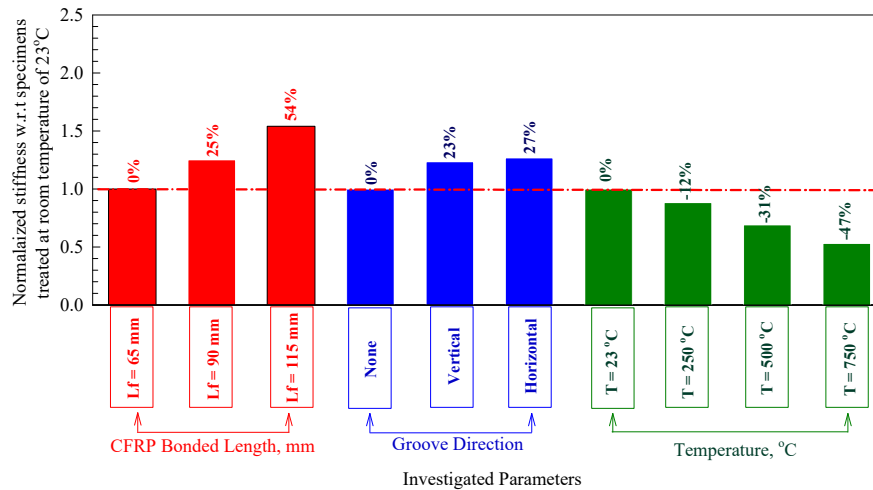


Figure 8. Normalized stiffness.

3.6. Toughness

The values of each sample's toughness were computed by determining the under-curve area of the bond force–slippage curve (Table 1). Then, the obtained toughness values were compared to the control specimen, which had no anchored grooves, as illustrated in Figure 9. Figure 9 shows that the increase in the length of the CFRP sheet was 38% (90 mm) and 77% (115 mm), which enhanced the toughness to 71 and 97%, respectively, with an enhancement rate of 1.94% per 1 mm of CFRP bonded length. The average improvement percentages of toughness were 71 and 201% for the specimens with grooves directed vertically and horizontally, respectively. Moreover, the percentages of reduction were 14, 49, and 73% for specimens treated at temperatures of 250, 500, and 750 °C, respectively, with an average toughness reduction of 1.48% for each 1 °C. Therefore, when exposed to extreme heat, the structures strengthened by CFRP sheets and anchored by horizontal grooves showed a great improvement in the structure's energy absorption and its capacity to deform plastically from the instant of de-bonding up to the point of ultimate bond force. It must be stated that toughness is the most remarkable parameter for its role in enhancing the percentages of improvement.

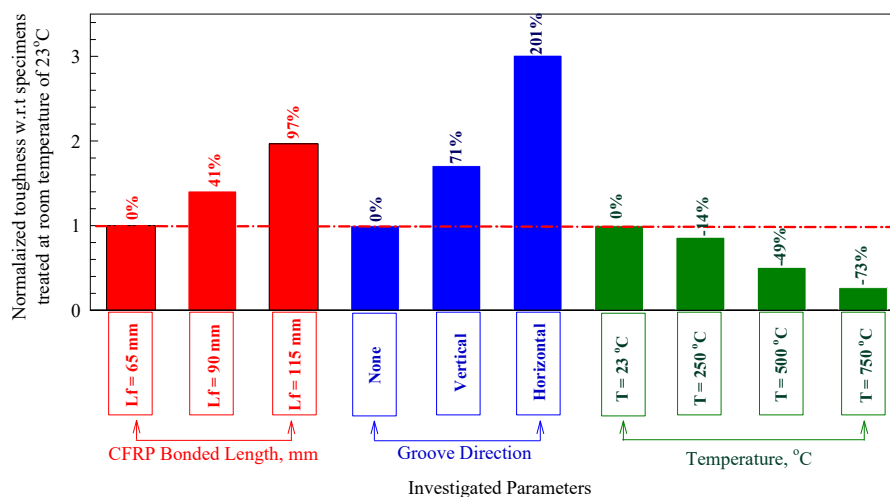


Figure 9. Normalized toughness.

4. Conclusions

The following conclusions can be drawn from this study:

- (1) The de-bonding failure of the specimens without anchored grooves and with vertical grooves was either through peeling-off of the concrete or shearing in the concrete surface. With the increase in horizontal grooves, the bond was enhanced in strength, as was evident from the amount of concrete left hanging onto the CFRP sheets when the surface failed in adhesion.
- (2) The bond force–slippage curve is split into two sections. The first is from the point of no zero loading up to the point of the emergence of CFRP de-bonding. The other section of the curve represents the point of the CFRP delamination from the bonded surface, in which the load is practically persistent, with promptly increasing slippage.
- (3) Utilizing the anchoring grooves improves, to a great extent, the behavior of the CFRP–concrete bond. With horizontal grooves, the improvement in the bond strength was around 36%, and this percentage was almost two times the enhancement achieved with vertical grooves.
- (4) This study has proven experimentally that horizontal grooves provide a great enhancement in ultimate slippage and bond strength. Therefore, the method of installing CFRP sheets and horizontal grooves lead to an adequate mode of failure.
- (5) Using the groove method has proven its practicality and cost-effectiveness. Since the epoxy performance is improved based on the groove direction, it is recommended to use horizontal grooves and CFRP sheets to restore the specimen’s original integrity, before de-bonding of CFRP and after attainment of ultimate bond strength.
- (6) It has been shown in this study that increasing the length of the bonded CFRP sheets increases the strength of the bond and enhances the ultimate slippage. The reason for these enhancements could be that, when increasing the length, there is an increase in the induced stresses generated by the exerted load. Moreover, the system becomes more uniform when the concentration of stresses is minimized.

Author Contributions: Conceptualization, R.A.-R. and M.A.-T.; methodology, R.A.-R. and M.A.-T.; formal analysis, R.A.-R. and M.A.-T.; investigation, R.A.-R. and M.A.-T.; resources, R.A.-R. and M.A.-T.; data curation, R.A.-R. and M.A.-T.; writing—original draft preparation, R.A.-R.; writing—review and editing, R.A.-R. and M.A.-T.; visualization, R.A.-R.; supervision, R.A.-R.; project administration, R.A.-R.; funding acquisition, R.A.-R. Both authors have read and agreed to the published version of the manuscript.

Funding: This research was funded by the Deanship of Research at Jordan University of Science and Technology, grant number 2018/265, and the APC was funded by the Deanship of Research at Jordan University of Science and Technology.

Acknowledgments: This work was fully supported by a grant from the Deanship of Research at Jordan University of Science and Technology (Project No. 2018/265). This support is gratefully acknowledged.

Conflicts of Interest: The authors declare no conflict of interest.

References

1. Bywalski, C.; Drzazga, M.; Kamiński, M.; Kaźmierowski, M. A New Proposal for the Shear Strength Prediction of Beams Longitudinally Reinforced with Fiber-Reinforced Polymer Bars. *Buildings* **2020**, *10*, 86. [[CrossRef](#)]
2. Triantafyllou, G.; Rousakis, T.C.; Karabinis, A. Corroded RC Beams at Service Load before and after Patch Repair and Strengthening with NSM CFRP Strips. *Buildings* **2019**, *9*, 67. [[CrossRef](#)]
3. Spinella, N.; Colajanni, P.; Recupero, A.; Tondolo, F. Ultimate Shear of RC Beams with Corroded Stirrups and Strengthened with FRP. *Buildings* **2019**, *9*, 34. [[CrossRef](#)]
4. Fathalla, E.; Salem, H. Parametric Study on Seismic Rehabilitation of Masonry Buildings Using FRP Based upon 3D Non-Linear Dynamic Analysis. *Buildings* **2018**, *8*, 124. [[CrossRef](#)]
5. Manie, S.; Jami, E.; Azarian, Z. Simplified Design of FRP-Confined Square RC Columns under Bi-Axial Bending. *Buildings* **2017**, *7*, 74. [[CrossRef](#)]
6. Al-Rousan, R.Z. Behavior of macro synthetic fiber concrete beams strengthened with different CFRP composite configurations. *J. Build. Eng.* **2018**, *20*, 595–608. [[CrossRef](#)]

7. Al-Rousan, R.Z.; Alhassan, M.A.; Alshuqari, E.A. Shear Nonlinear Behavior of plain concrete beams with DSSF strengthened in flexure with anchored CFRP sheets—Effects of DSSF content on the bonding length of CFRP sheets. *Case Stud. Constr. Mater.* **2018**, *9*, e195.
8. Haddad, R.H.; Al-Rousan, R.Z.; Ghanma, L.; Nimri, Z. Modifying CFRP–concrete bond characteristics from pull-out testing. *Mag. Concr. Res.* **2015**, *67*, 707–717. [[CrossRef](#)]
9. Al-Rousan, R.Z. Empirical and NLFEA prediction of bond-slip behavior between DSSF concrete and anchored CFRP composites. *Constr. Build. Mater.* **2018**, *169*, 530–542. [[CrossRef](#)]
10. Haddad, R.H.; Al-Rousan, R.Z.; Almasry, A. Bond-slip behavior between carbon fiber reinforced polymer sheets and heat-damaged concrete. *Compos. Part B Eng.* **2013**, *45*, 1049–1060. [[CrossRef](#)]
11. Al-Rousan, R.Z.; Al-Saraireh, S. Impact of anchored holes technique on behavior of reinforced concrete beams strengthened with different CFRP sheet lengths and widths. *Case Stud. Constr. Mater.* **2020**, *13*, e00405. [[CrossRef](#)]
12. Al-Rousan, R.Z.; Al-Tahat, M.F. Consequence of surface preparation techniques on the bond behavior between concrete and CFRP composites. *Constr. Build. Mater.* **2019**, *212*, 362–374. [[CrossRef](#)]
13. Haddad, R.H.; Al-Rousan, R.Z. An anchorage system for CFRP strips bonded to thermally shocked concrete. *Int. J. Adhes. Adhes.* **2016**, *71*, 10–22. [[CrossRef](#)]
14. ACI (American Concrete Institute). *Guide Test Methods for Fiber Reinforced Polymers (FRPs) for Reinforcing or Strengthening Concrete Structures*; ACI 4403R-12; American Concrete Institute: Farmington Hills, MI, USA, 2012.
15. Fib Task Group. *Externally Bonded FRP Reinforcement for RC Structures, 9.3*; International Federation for Structural Concrete: Lausanne, Switzerland, 2001.
16. ACI (American Concrete Institute). *Guide for the Design and Construction of Externally Bonded FRP Systems for Strengthening Concrete Structures*; ACI 4402R-17; American Concrete Institute: Farmington Hills, MI, USA, 2017.
17. International Concrete Repair Institute. *Selecting and Specifying Concrete Surface Preparation for Sealers, Coatings and Polymer Overlays*; ICRI 3102R-2013; ICRI: St. Paul, MN, USA, 2013.
18. De Lorenzis, L.; Miller, B.; Nanni, A. Bond of Fiber-Reinforced Polymer Laminates to Concrete. *ACI Mater. J.* **2001**, *98*, 256–264. [[CrossRef](#)]
19. Toutanji, H.; Ortiz, G. The effect of surface preparation on the bond interface between FRP sheets and concrete members. *Compos. Struct.* **2001**, *53*, 457–462. [[CrossRef](#)]
20. Chajes, M.J.; Finch, W.W.; Thomson, T.A. Bond and Force Transfer of Composite-Material Plates Bonded to Concrete. *ACI Struct. J.* **1996**, *93*, 208–217. [[CrossRef](#)]
21. Biscaia, H.C.; Micaelo, R.; Teixeira, J.; Chastre, C. Numerical analysis of FRP anchorage zones with variable width. *Compos. Part B Eng.* **2014**, *67*, 410–426. [[CrossRef](#)]
22. Iovinella, I.; Prota, A.; Mazzotti, C. Influence of surface roughness on the bond of FRP laminates to concrete. *Constr. Build. Mater.* **2013**, *40*, 533–542. [[CrossRef](#)]
23. Ueda, T.; Dai, J.G. Interface bond between FRP sheets and concrete substrates: Properties, numerical modeling and roles in member behaviour. *Prog. Struct. Eng. Mater.* **2005**, *7*, 27–43. [[CrossRef](#)]
24. Mostofinejad, D.; Kashani, A.T. Experimental study on effect of EBR and EBROG methods on debonding of FRP sheets used for shear strengthening of RC beams. *Compos. Part B Eng.* **2013**, *45*, 1704–1713. [[CrossRef](#)]
25. Moshiri, N.; Tajmir-Riahi, A.; Mostofinejad, D.; Czaderski, C.; Motavalli, M. Experimental and analytical study on CFRP strips-to-concrete bonded joints using EBROG method. *Compos. Part B Eng.* **2019**, *158*, 437–447. [[CrossRef](#)]
26. Mostofinejad, D.; Mahmoudabadi, E. Grooving as Alternative Method of Surface Preparation to Postpone Debonding of FRP Laminates in Concrete Beams. *J. Compos. Constr.* **2010**, *14*, 804–811. [[CrossRef](#)]
27. Hong, S.; Park, S.-K. Effect of prestress and transverse grooves on reinforced concrete beams prestressed with near-surface-mounted carbon fiber-reinforced polymer plates. *Compos. Part B Eng.* **2016**, *91*, 640–650. [[CrossRef](#)]
28. Jiang, C.; Wan, B.; Wu, Y.F.; Omboko, J. Epoxy interlocking: A novel approach to enhance FRP-to-concrete bond behavior. *Constr. Build. Mater.* **2018**, *193*, 643–653. [[CrossRef](#)]
29. Chen, C.; Li, X.; Wang, X.; Sui, L.; Xing, F.; Li, D.; Zhou, Y. Effect of transverse groove on bond behavior of FRP-concrete interface: Experimental study, image analysis and design. *Compos. Part B Eng.* **2019**, *161*, 205–219. [[CrossRef](#)]

30. Hosseini, A.; Mostofinejad, D. Effect of groove characteristics on CFRP-to-concrete bond behavior of EBROG joints: Experimental study using particle image velocimetry (PIV). *Constr. Build. Mater.* **2013**, *49*, 364–373. [[CrossRef](#)]
31. Hosseini, A.; Mostofinejad, D. Experimental investigation into bond behavior of CFRP sheets attached to concrete using EBR and EBROG techniques. *Compos. Part B Eng.* **2013**, *51*, 130–139. [[CrossRef](#)]
32. Biscaia, H.C.; Silva, M.A.G.; Chastre, C. Factors influencing the performance of externally bonded reinforcement systems of GFRP-to-concrete interfaces. *Mater. Struct.* **2015**, *48*, 2961–2981. [[CrossRef](#)]
33. Lu, X.Z.; Teng, J.G.; Ye, L.P.; Jiang, J.J. Bond-slip models for FRP sheets/plates bonded to concrete. *Eng. Struct.* **2005**, *27*, 920–937. [[CrossRef](#)]
34. Dai, J.; Ueda, T.; Sato, Y. Development of the nonlinear bond stress-slip model for fiber reinforced plastics sheet-concrete interfaces with a simple method. *J. Compos. Constr.* **2005**, *9*, 52–62. [[CrossRef](#)]
35. Nakaba, K.; Toshiyuki, K.; Tomoki, F.; Hiroyuki, Y. Bond Behavior between Fiber-Reinforced Polymer Laminates and Concrete. *ACI Struct. J.* **2001**, *98*, 359–367. [[CrossRef](#)]
36. Chen, C.; Sui, L.L.; Xing, F.; Li, D.W.; Zhou, Y.W.; Li, P.D. Predicting bond behavior of HB FRP strengthened concrete structures subjected to different confining effects. *Compos. Struct.* **2018**, *187*, 212–225. [[CrossRef](#)]
37. Bazant, Z.; Kaplan, M. *Concrete at High Temperatures: Material Properties and Mechanical Models*; Longman Group Limited: London, UK, 1996.
38. Lawson, J.R.; Phan, L.T.; Davis, F. *Mechanical Properties of High Performance Concrete after Exposure to Elevated Temperatures*; Report Submitted to National Institute and Standards and Technology, IR 6475; National Institute and Standards and Technology: Gaithersburg, MD, USA, 2000.
39. Dima, M.A. Thermal Mechanical Behavior of Confined Fibrous Lightweight Aggregate Concrete. Master's Thesis, Department of Civil and Materials Engineering, Jordan University of Science and Technology, Ar-Ramtha, Jordan, 2007.
40. *ASTM C33/C33M-18: Standard Specification for Concrete Aggregates*; ASTM International: West Conshohocken, PA, USA, 2018. Available online: www.astm.org (accessed on 6 December 2020).
41. Alhassan, M.A.; Al-Rousan, R.Z.; Abu-Elhija, A.M. Anchoring holes configured to enhance the bond-slip behavior between CFRP composites and concrete. *Constr. Build. Mater.* **2020**, *250*, 118905. [[CrossRef](#)]

Publisher's Note: MDPI stays neutral with regard to jurisdictional claims in published maps and institutional affiliations.



© 2020 by the authors. Licensee MDPI, Basel, Switzerland. This article is an open access article distributed under the terms and conditions of the Creative Commons Attribution (CC BY) license (<http://creativecommons.org/licenses/by/4.0/>).